Available online at www.sciencedirect.com

SciVerse ScienceDirect

Journal of the European Ceramic Society 32 (2012) 2971–2979

www.elsevier.com/locate/jeurceramsoc

Co-precipitation synthesis route to yttrium aluminum garnet (YAG) transparent ceramics

Jiang Li [a,*], Feng Chen [b], Wenbin Liu [a], Wenxin Zhang [a], Liang Wang [a], Xuewei Ba [a], Yingjie Zhu [b], Yubai Pan [a], Jingkun Guo [a,b]

[a] *Key Laboratory of Transparent Opto-fuctional Inorganic Materials, Shanghai Institute of Ceramics, Chinese Academy of Sciences, Shanghai 200050, China*
[b] *State Key Laboratory of High Performance Ceramics and Superfine Microstructure, Shanghai Institute of Ceramics, Chinese Academy of Sciences, Shanghai 200050, China*

Available online 20 March 2012

Abstract

Yttrium aluminum garnet (YAG) precursor was synthesized via a coprecipitation method with aluminum nitrate and yttrium nitrate as raw materials, using ammonium hydrogen carbonate (AHC) as the precipitant. Fine and low-agglomerated YAG powder was obtained by calcining the precursor at 1200 °C. The primary crystallites were measured to be ∼120 nm in size and weakly agglomerated to a particle size of ∼500 nm, indicating a high degree of sinterability. With 0.5 wt% tetraethyl orthosilicate (TEOS) and 0.1 wt% magnesia as sintering aids, transparent YAG ceramics were fabricated by vacuum sintering at 1730–1790 °C for various hours. The influences of sintering temperature and holding time on the microstructure and transmittance of YAG ceramics were discussed.

Keywords: Transparent ceramics; YAG powders; Vacuum sintering; Co-precipitation synthesis

1. Introduction

Coble first demonstrated that polycrystalline ceramics could be sintered to a visually transparent/translucent state and translucent alumina ceramics (Lucalox) were prepared.[1,2] Since then, a variety of transparent/translucent ceramics including MgO,[3] Y_2O_3,[4] $MgAl_2O_4$,[5] PLZT,[6] AlON,[7] SiAlON,[8] AlN,[9] YAG[10] have been successfully produced by sintering to exceptionally high densities and thus reducing/eliminating light scattering from residual porosity. Transparent YAG ceramics hold promise for certain optical applications such as solid-state laser host media, luminous pipes for high-intensity discharge lamps or heat-resistive windows because of their large doping concentrations,[11,12] increased compositional and structural versatility,[13–15] good chemical corrosion resisitivity,[16] and high mechanical property.[17]

Usually, two source powders are utilized to make YAG transparent ceramics: (i) mixtures of Y_2O_3 and Al_2O_3, which form YAG in situ during solid-state reactive sintering,[18–24] and (ii) wet-chemical synthesized YAG powder.[25–29] Solid-state reactive sintering is a relatively simple way to fabricate YAG transparent ceramics and a range of compositions is easy to implement by changing the reactant powder amounts during batching.[30,31] However, the incorporation of some impurities is unavoidable during ball milling. Wet chemical approaches such as precipitation,[32–36] spray pyrolysis,[37,38] hydrothermal (or solvothermal) synthesis,[39–41] sol–gel[42–44] and combustion synthesis[45–49] have many advantages such as atomic level mixing of high-purity precursors and low processing temperature. Among the wet chemical methods, precipitation is a relatively simple way to synthesize YAG powder with composition homogeneity, good crystallinity and pure phase at low temperature. And fully dense and transparent ceramics can be fabricated by vacuum sintering of YAG powders with high sinterability.

In this paper, carbonate precursors of YAG were synthesized via a coprecipitation method using ammonium hydrogen carbonate (AHC) as the precipitant. Nanosized YAG powders with high sinterability were obtained at 1200 °C and transparent YAG ceramics were fabricated by vacuum sintering at 1730–1790 °C with a considerable amount of additives of tetraethoxysilane (TEOS) and MgO.

* Corresponding author.
E-mail address: lijiang@mail.sic.ac.cn (J. Li).

0955-2219/$ – see front matter © 2012 Elsevier Ltd. All rights reserved.
doi:10.1016/j.jeurceramsoc.2012.02.040

2. Experimental

2.1. Materials

Several raw materials were used to synthesize nanosized YAG powders: yttria (Y_2O_3, Shanghai Yuelong New Materials Co. Ltd., China, 99.99% purity), aluminum nitrate nonahydrate ($Al(NO_3)_3{\cdot}9H_2O$, Sigma–Aldrich Chemicals, USA, >98% purity), ammonium hydrogen carbonate (NH_4HCO_3, Sigma–Aldrich Chemicals, USA, >99% purity) and ammonium sulfate ($(NH_4)_2{\cdot}SO_4$, Sinopharm Chemical Reagent Co. Ltd., China, analytical purity).

2.2. Powder synthesis

In the present work, a wet-chemical synthesis route was utilized to produce nanosized YAG powders, employing $Al(NO_3)_3{\cdot}9H_2O$ and Y_2O_3 as the starting materials, respectively. Yttrium nitrate solution was prepared by dissolving the yttria powder in the heated nitric acid (Shanghai Lingfeng Chemical Reagent Co., Ltd., super-high purity). Aluminum nitrate solution was prepared by dissolving the $Al(NO_3)_3{\cdot}9H_2O$ in the deionized water. Al^{3+} and Y^{3+} concentrations of the nitrate solutions were assayed by the ICP (Inductively Coupled Plasma) spectrophotometric technique. The metal nitrates were mixed to meet the YAG stoichiometry and further adjusted the solution concentration to 0.19 M for Al^{3+}. As a precipitation solution, a 0.92 M solution of ammonium hydrogen carbonate (AHC) was used and ammonium sulfate (0.11 g in 100 ml of deionized water) was added to the solution. The precursor precipitate was made at the room temperature by dripping 2200 ml of ammonium hydrogen carbonate solution into 1100 ml of the mixed solution of mother nitrate salts at a speed of 2 ml/min under mild agitation and the final pH value of the slurry was about 8.0. The resultant suspension was agitated for 6 h and aged for 12 h. Then, the suspension was filtered using centrifugal filtration, washed four times with deionized water, rinsed twice with ethanol, and dried at 70 °C for 24 h. The dried cake was crushed with a corundum pestle and mortar, and sieved through a 200-mesh screen. The sieved precursor powder was calcined at different temperatures for 3 h to form garnet phase of YAG powders.

2.3. Powder characterization

Thermal gravimetric analysis and differential thermal analysis (TG–DTA) of the original precursor were recorded on a Netzsch STA 449C Instrument. Measurements were taken under a continuous flow of air (20 ml/min). Sample was heated at 10 °C/min to 1400 °C and then cooled to room temperature naturally.

Chemical analysis was made to confirm the chemical stoichiometry of YAG powders. Y and Al contents were determined by the chelate-titrimetric method.

Phase identification was performed by the X-ray diffraction (XRD) method on a HUBER Imaging Plate Guinier Camera G670 [S] ($CuK_{\alpha 1}$ radiation, $\lambda = 1.54056$ Å, 40 kV/30 mA, Ge monochromator). The 2θ for all data ranged from 15° to 65° with 0.005° step size. The average crystallite size of the calcined powders was calculated from X-ray peak broadening using Scherrer formula. The XRD data are refined by Rietveld method using the Jade program (Version 5.0).

Specific surface area analyses were conducted at 77 K using a Norcross ASAP 2010 micromeritics, with N_2 as the absorbate gas. Powders were degassed at 150 °C until the air pressure was below 5 μm Hg. The specific surface areas were calculated using the BET multipoint method with 8 data points. The average particle size of the calcined powders was calculated from the specific surface area data.

Microstructures were observed on a JEOL JSM-6700 FESEM and the mean particle size was estimated by measuring diameters of 100 particles in the FESEM photographs. Powders were dispersed in ethanol using an ultrasonic horn. Drops of the dispersed materials were deposited on a copper stub and dried in nature. Samples were sputter coated with palladium using a JEOL JFC-1600 auto fine coater system.

The agglomeration particle size distribution was measured by a dynamic laser scattering (DLS) method on a Brookhaven ZetaPlus Zeta Potential Analyzer.

2.4. Ceramic fabrication and characterization

Using the powder calcined at 1200 °C as starting materials, 0.5 wt% TEOS (Alfa Aesar, 99.999% purity, USA) and 0.1at%MgO (Sinopharm Chemical Reagent Co., Ltd., spectral purity, China) as sintering aids, two powder batches were ball milled in anhydrous ethanol for 10 h using high-purity (99.7%) alumina balls and the balling media had no measurable weight loss after milling. The milled suspensions were dried at 90 °C in an oven and ground in an alumina mortar. After sieving through 200-mesh screen, two powder batches were uniaxially pressed in a 20 mm die at 10 MPa followed by cold isostatical pressing (CIP) at 250 MPa. The compacted disks were sintered at the temperature range of 1730–1790 °C up to 30 h in a tungsten mesh heated vacuum furnace (KZG-110F, Shanghai Chenrong Electrical Furnace Co., Ltd., Shanghai, China) under 3×10^{-3} Pa vacuum during holding. The heating and cooling rates were 5 °C/min and 10 °C/min, respectively. All the sintered specimens were annealed at 1450 °C for 20 h in air to remove the oxygen vacancies. For optical transmission comparison, YAG transparent ceramics were also fabricated by a solid-state reactive sintering method[20] using commercial Y_2O_3 and α-Al_2O_3 powders as starting materials.

Densities of the sintered specimens were measured by the Archimedes method, using deionized water as the immersion medium. Microstructures of the fractured surfaces and the polished and thermal-etched surfaces were observed by EPMA (Model JXA-8100, JEOL, Japan). Mirror-polished specimens on both surfaces with the thickness of 1.0 mm were used to measure the optical in-line transmittance (Model Cray-5000 UV-VIS-NIR Spectrophotometer, Varian, CA, USA).

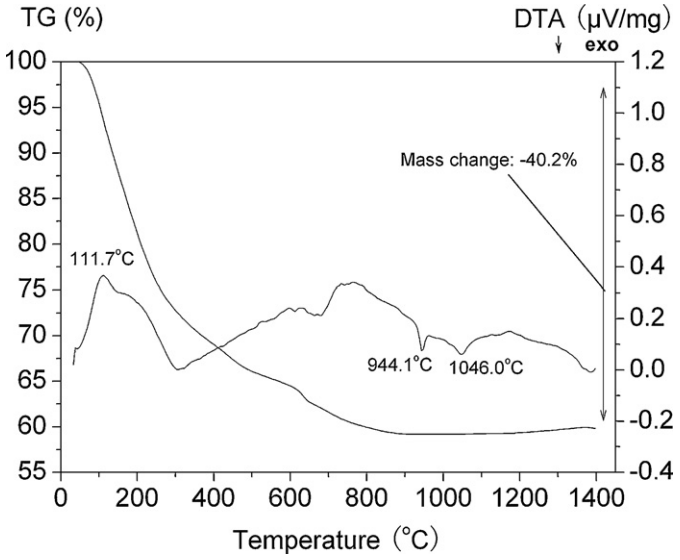

Fig. 1. TG–DTA curves of the precursor produced by AHC coprecipitation method.

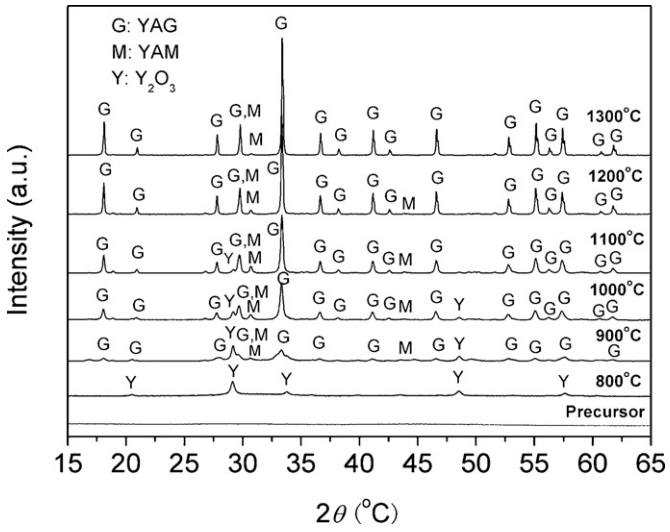

Fig. 2. XRD patterns of as-synthesized precursor and the resultant powders obtained by calcining the precursors at different temperatures for 3 h.

3. Results and discussion

The concentration of ammonium hydrogen carbonate solution was considered to affect composition of the resultant precipitate. Previous work[50] revealed that Al^{3+} ions may precipitate as pseudo-boehmite (AlOOH) or ammonium dawsonite [($NH_4Al(OH)_2CO_3$)] mainly depending on the concentration of AHC solution. On the other hand, Y^{3+} may most likely precipitate as normal carbonate of [$Y_2(CO_3)_3{\cdot}nH_2O$ ($n=2$–3)][51] or basic carbonate of [$Y(OH)CO_3$][52] from the present carbonate anions containing AHC solution. The direct formation of yttrium normal carbonate rather than basic carbonate was mainly due to the high CO_3^{2-} concentration of the AHC solution. Yttrium basic carbonate of [$Y(OH)CO_3$] was classically produced by the so-called homogeneous precipitation process achieved by the forced hydrolysis of urea at elevated temperature (>83 °C). In this experiment, concentration of the AHC solution was selected as 0.92 M. Al^{3+} ions precipitated from solution of nitrate as (AlOOH) and [($NH_4Al(OH)_2CO_3$)]. If we regard the number of crystallization water of $Y_2(CO_3)_3{\cdot}nH_2O$ as 3 according to the previous work,[53] the composition of the obtained precursor can be described as $10[x(NH_4Al(OH)_2CO_3){\cdot}(1-x)AlOOH]{\cdot}3[Y_2(CO_3)_3{\cdot}3H_2O]$.

TG–DTA curves of the precursor show two endothermic and two exothermic peaks up to 1400 °C, with a total weight loss of ~40.2%, as shown in Fig. 1. This weight loss is regarded as the theoretical mass of a precursor with an approximate composition of $10[0.19(NH_4Al(OH)_2CO_3){\cdot}0.81AlOOH]{\cdot}3[Y_2(CO_3)_3{\cdot}3H_2O]$. According to the chemical analysis result, it was found the mole ratio of Y to Al was 0.593, which was a little less than the stoichiometric value. So it can be considered that a relatively accurate composition of the precursor is $10[0.19(NH_4Al(OH)_2CO_3){\cdot}0.81AlOOH]{\cdot}3[Y_{1.9767}(CO_3)_3{\cdot}3H_2O$. The weight loss of the precursor at lower temperature (<400 °C) was mainly ascribed to the release of ammonia and molecular water and the partial decomposition of CO_3 group, while that occurred at higher temperature (>400 °C) was mainly due to the further decomposition of carbonate species.[35] The relatively sharper endothermic peak located at ~112 °C was assigned to the evaporation of absorbed water. The relatively wider endothermic peak at ~150 °C may be caused by the release of molecular water and the decomposition of $NH_4Al(OH)_2CO_3$. The exothermic peaks at 944 °C and 1046 °C were caused by the crystallization of yttrium aluminum monoclinic ($Y_4Al_2O_9$, YAM) and YAG phases, respectively. This observation was confirmed by the XRD results given in Fig. 2.

Fig. 2 shows the XRD patterns of as-synthesized precursor and the resultant powders obtained by calcining the precursors at different temperatures for 3 h. The co-precipitated powder was found to be amorphous. For the powder calcined at 800 °C, cubic Y_2O_3 (JCPDS 89-5592) and amorphous Al_2O_3 formed. Monoclinic YAP (JCPDS 16-219) and cubic YAG (JCPDS 82-0575) crystallized at 900 °C with the presence of Y_2O_3 phase. At 1000 °C and 1100 °C, the YAP and Y_2O_3 phases persisted, but with increase of intensity for YAP and with loss of intensity for Y_2O_3 as more YAG formed. Calcining to 1200 °C and 1300 °C resulted in an almost-complete conversion to YAG, and only a very small amount of YAM remained. The results are not consistent with the observations of Li et al.,[35] in which direct crystallization of YAG phase occurred at 900 °C without the formation of any intermediate phases. In Li's work,[35] YAG precursor was obtained by adding nitrate solution to the AHC precipitant solution, which was called as the reverse-strike method. In the present work, chemical precipitation was performed by the normal-strike method (adding AHC precipitant solution to the nitrate solution). The main deference between the two methods is the rate at which pH of the nitrate solution change as a function of time. For multi-cation material of YAG, the former technique has the advantage of high cation homogeneity in the precursor. However, it suffers from the disadvantage of aggregation at relatively high pH value of precipitant solution. For the normal-strike method, the cation distribution in

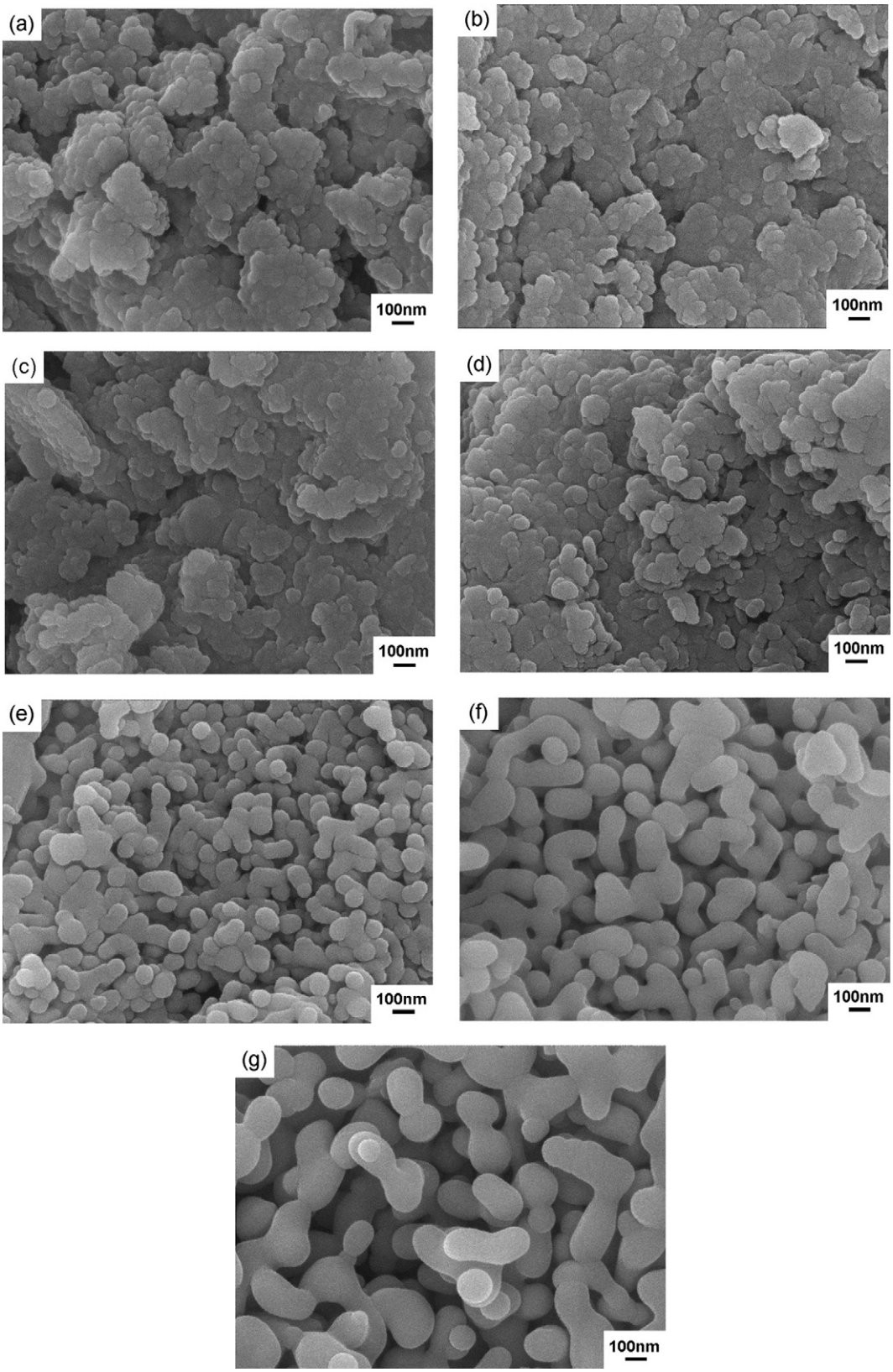

Fig. 3. FESEM micrographs of as-synthesized precursor and the resultant powders obtained by calcining the precursors at different temperatures for 3 h: (a) precursor; (b) 800 °C; (c) 900 °C; (d) 1000 °C; (e) 1100 °C; (f) 1200 °C; and (g) 1300 °C.

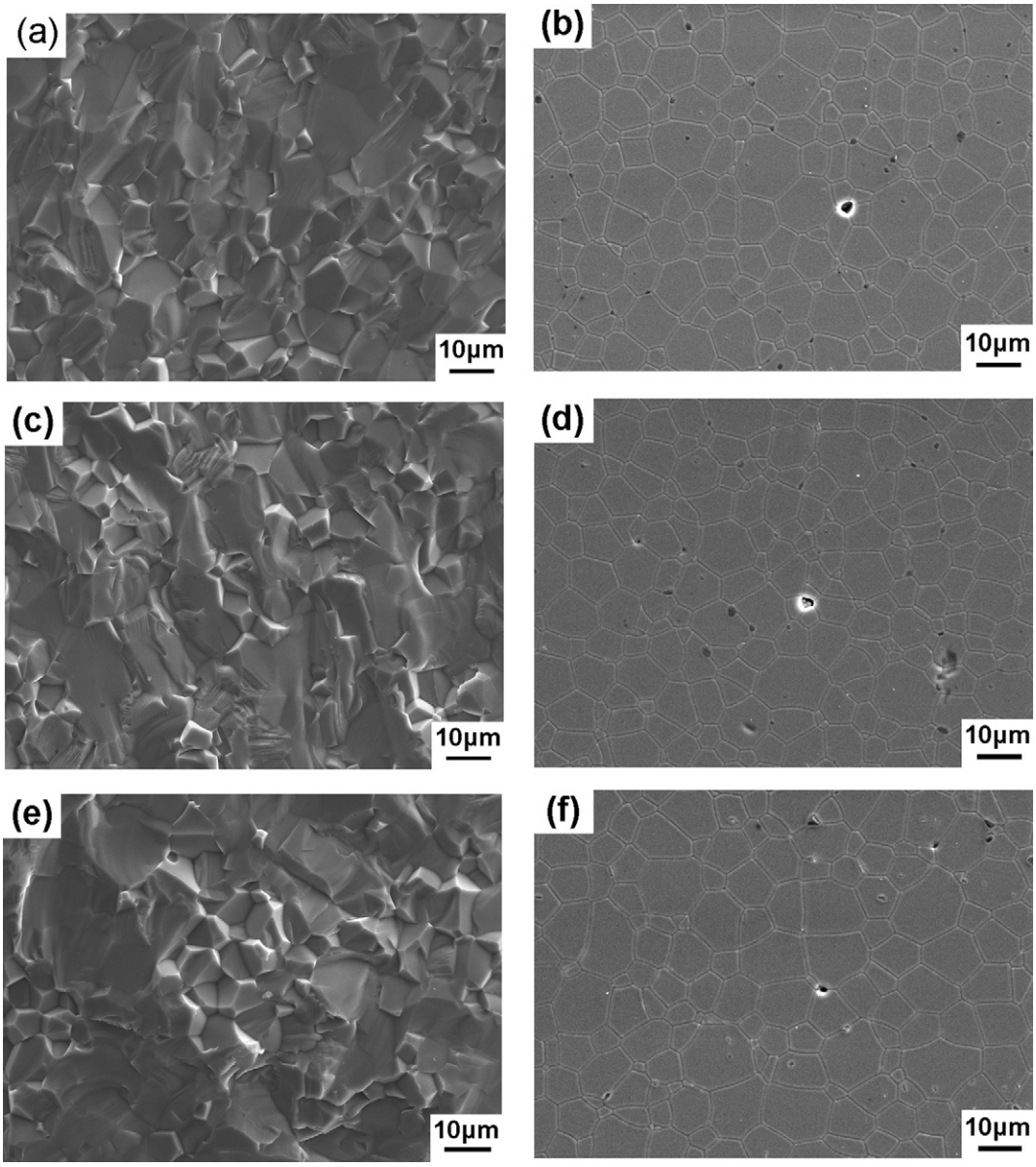

Fig. 4. SEM micrographs of the fractured surfaces and the mirror-polished and thermal etched surfaces of YAG ceramics sintered at (a and b) 1730 °C, (c and d) 1760 °C and (e and f) 1790 °C for 10 h.

the precursor is not as homogenous as that prepared by reverse-strike method, as can be confirmed by XRD results in Fig. 2. Nevertheless, precipitation reaction occurred at relatively warm condition, so the dispersion property of the particle synthesize by the normal-strike method is better for the reverse-strike method. The mean crystallite size of YAG powder defined as D_{XRD} was determined by X-ray line broadening and calculated using the Scherrer equation:

$$D_{XRD} = \frac{0.89\lambda}{B \cos \theta}$$

where $B = (B_o^2 - B_c^2)^{1/2}$, B_o is the full width at half maximum (in° 2θ), B_c is the correction factor for instrument broadening, θ is the angle of the peak maximum (in° 2θ), and λ is the CuK_α weighted average wavelength. For the powders calcined at 1000, 1100, 1200 and 1300 °C, the mean crystallite size values of YAG powders calculated from the (2 1 1) XRD peaks are 39, 49, 101 and 135 nm, respectively.

Fig. 3 shows the FESEM micrographs of as-synthesized precursor and the resultant powders obtained by calcining the precursors at different temperatures for 3 h. The precursor mainly contains sub-micrometer sized aggregates of nano-sized primary particles. The resultant powders calcined at 800, 900 and 1000 °C were agglomerated and showed similar overall morphology to that of the precursor. For the powders calcined at 1100, 1200 and 1300 °C, appreciable particle growth from 70 nm to 120 nm and 150 nm occurred with increasing the calcination temperature. The mean primary particle size estimated from FESEM photographs is denoted as D_{FESEM}. The mean agglomerate size D_{50} is the median diameter determined from the particle size distribution measured by the dynamic laser scattering (DLS) method. The D_{50} value of the resultant powder

calcined at 1200 °C is about 500 nm. The particle size D_{BET} was calculated from the following formula

$$D_{BET} = \frac{6}{\rho \cdot S_{BET}}$$

where ρ (4.55 g/cm^3) is the theoretical density of YAG, and S_{BET} is the specific surface area determined by BET measurement. The measured particle size of D_{BET} for the YAG is about 115 nm. It can be found that the D_{SEM} value of the YAG powder is just a little larger than that of D_{XRD}. This indicates that each particle shown in the FESEM photograph is a single crystallite. The measured value of D_{BET} is nearly the same as the mean particle size in FESEM micrograph. The agreement of D_{BET} with D_{FESEM} of the powder indicates that the secondary particles with mean diameter of ~500 nm have porous structure, in which the primary particles with mean diameter of 120 nm are weakly agglomerated by small connections with necks.

According to the above analysis, it is considered that the resultant powder calcined at 1200 °C will be favorable for transparent ceramic fabrication. Higher calcination temperature caused drastic increase in crystallite size and decrease in sinterability. While the YAG powders produced at lower temperature, though have smaller crystallite sizes, had more secondary phases and exhibited lower densification rates. The YAG powder was sintered to over 99% of theoretical density at above 1700 °C. Fig. 4 shows the SEM micrographs of the fractured surfaces and the mirror-polished and thermal etched surfaces of YAG ceramics sintered at 1730, 1760 and 1790 °C for 10 h. It can be seen that the sintered bodies have homogeneous structures and the grain size increases from 8.5 to 9.1 μm and 9.9 μm with increase of sintering temperature. All the specimens have a few pores remained mainly at the grain boundaries. The formed secondary phase corresponding to alumina is caused by the nonstoichiometry of the YAG powder, in which the mole ratio of Y to Al (0.593) determined by chemical analysis is lower than theoretical value of 0.6.

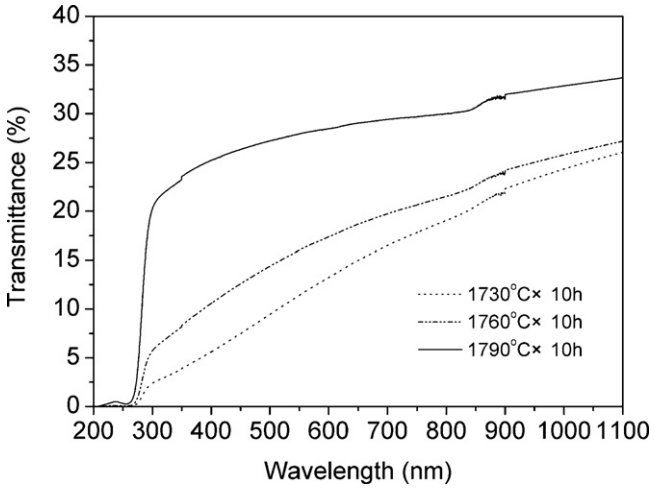

Fig. 5. In-line transmittance of the transparent YAG ceramics from powder sintered at 1730, 1760 and 1790 °C for 10 h.

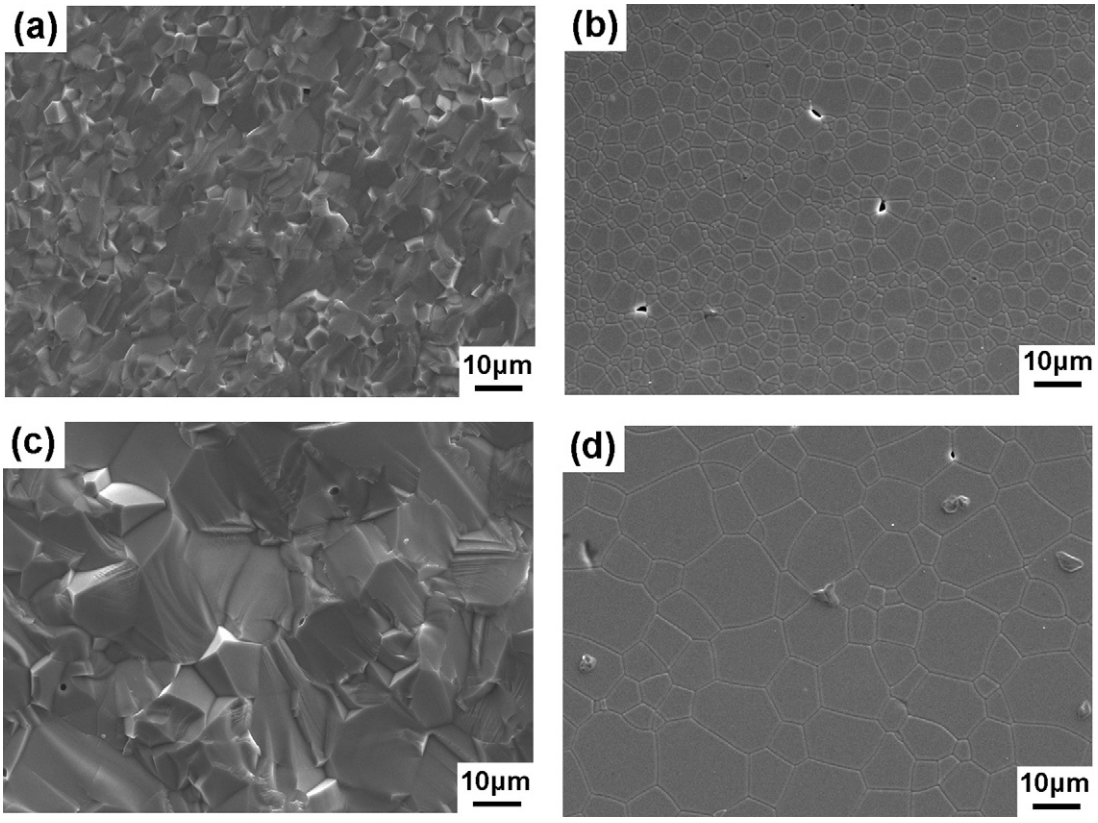

Fig. 6. SEM micrographs of the fractured surfaces and the mirror-polished and thermal etched surfaces of YAG ceramics from powder sintered at 1790 °C for (a and b) 2 h and (c and d) 20 h.

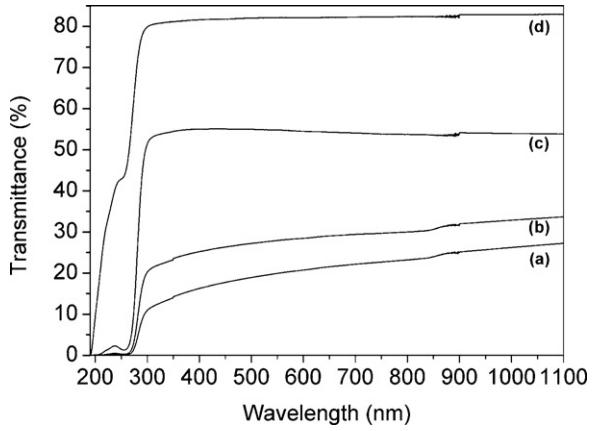

Fig. 7. In-line transmittance of 1 mm-thick YAG transparent ceramics from powder sintered at 1790 °C for (a) 2 h, (b) 10 h, (c) 20 h, and (d) 2 mm-thick YAG transparent ceramic fabricated by a solid-state reactive sintering method.

Fig. 5 shows the optical in-line transmittance spectra of the 1 mm-thick transparent YAG ceramics sintered at 1730, 1760 and 1790 °C for 10 h. The in-line transmittance increases with increase of sintering temperature. For the sample sintered at 1790 °C for 10 h, the transmittance reached 33.4% at 1064 nm. However, the value of transmission is much lower than the theoretical value due to the existence of residual pores and secondary phase, as can be confirmed in Fig. 4.

Besides sintering temperature, holding time at maximum temperature also has an obvious effect on the microstructure and optical transmittance of YAG ceramic. Fig. 6 shows the SEM micrographs of the fractured surfaces and the mirror-polished and thermal etched surfaces of YAG ceramics sintered at 1790 for 2 and 20 h. Both sintered bodies have homogeneous microstructures with grains ~4.0 and 11.9 μm in diameter as far as the SEM photographs show. Micro-pores were gradually removed with increasing the holding time. However, there are still a few residual pores remained at triple junctions or along grain boundaries even at the holding time as long as 20 h.

Fig. 7 shows the in-line transmittance spectra of YAG transparent ceramics from powder sintered at 1790 °C for 2, 10 and 20 h, as well as the specimen fabricated by solid-state reactive sintering method. The in-line transmittance increases with increasing the holding time. However, even with the holding time of 20 h, the optical transmittance (~55% in the visible light region) of YAG transparent ceramic is far lower than that of the sample fabricated by solid-state reaction and vacuum sintering due to the existence of optical scattering. The main optical scattering was caused by not only the residual micro-pores, but also the secondary phase of alumina. The pores with the size of several microns present in the samples are likely a result of voids or pressure gradients during green forming. The single best way to remove such micro-pores is move towards a colloidal forming method. Slip casting, tape casting, gel-casting, etc. are all better suited to forming transparent ceramics than dry pressing because they are better able to handle nano-scaled powders and they produce more homogeneous green bodies.[54,55] When properly done, these methods lead to more evenly distributed pore size distributions and fewer defects. They are, of course, more difficult to handle than dry pressing. In the present work, the much more severe optical scattering is caused by the secondary phase of alumina. And the nonstoichiometry of the YAG powder is the origin of secondary phase. In order to keep the stoichiometry of the YAG powder prepared by co-precipitation method and vacuum sintering, every step of the process should be precisely controlled. In addition, sintering aid category and amount, as well as sintering schedule should be carefully taken into account to enhance the densification, control the grain size and optimize the microstructure of the sintered body.

4. Conclusions

The results of the present study can be summarized as follows:

(1) YAG precursor with the composition of $10[0.19(NH_4Al(OH)_2CO_3)\cdot 0.81AlOOH]\cdot 3[Y_{1.9767}(CO_3)_3\cdot 3H_2O$ was prepared by the coprecipitation method with aluminum nitrate and yttrium nitrate as raw materials, using ammonium hydrogen carbonate as the precipitant. Calcination of the precursor at 1200 °C resulted in fine and low-agglomerated YAG powder. The powder was measured to be ~120 nm in primary crystallite size and ~500 nm in agglomerate size. The agglomerate particles had a porous structure with a netlike connection.
(2) Nanosized YAG powders were sintered into transparent bodies by vacuum sintering at 1730–1790 °C with a considerable amount of TEOS and MgO additions. All the sintered YAG ceramics exhibited homogeneous microstructures with no abnormal grain growth.
(3) The in-line transmittance (~55% in the visible light wavelength) of the YAG ceramic sintered at 1790 °C for 20 h is far lower than that of the sample fabricated by solid-state reaction and vacuum sintering due to the existence of residual micro-pores and secondary phase.
(4) It is very important to synthesize a stoichiometric and low-agglomerated YAG powder by co-precipitation method for transparent ceramic fabrication.

Acknowledgements

Helpful discussions with Dr. Adam J. Stevenson are greatly appreciated. This work was supported by the Natural Science Foundation of Shanghai (Grant No. 10ZR1433900), the Project for Young Scientists Fund of National Natural Science Foundation of China (Grant No. 51002172), the Key Program of National Natural Science Foundation of China (Grant No. 91022035) and the Science and Technology Innovation Program of Shanghai Institute of Ceramics, Chinese Academy of Sciences (Grant No. Y12ZC3130G).

References

1. Coble RL. *Transparent alumina and method of preparation*. US Patent 3026210, March; 1962.

2. Coble RL. Sintering alumina: effect of atmospheres. *J Am Ceram Soc* 1962;**45**:123–7.
3. Miles GD, Sambell RAJ, Rutherford J, Stephenson GW. Fabrication of fully dense transparent polycrystalline magnesia. *Trans Br Ceram Soc* 1967;**7**:319–35.
4. Lefever RA, Matsko J. Transparent yttrium oxide ceramics. *Mater Res Bull* 1967;**9**:865–9.
5. Bratton RJ. Translucent sintered $MgAl_2O_4$. *J Am Ceram Soc* 1974;**57**:283–6.
6. Haertling GH, Land CE. Improved hot-pressed electrooptic ceramics in the (Pb,La)(Zr,Ti)O_3 system. *J Am Ceram Soc* 1971;**54**:303–9.
7. McCauley JW, Corbin ND. Phase relations and reaction sintering of transparent cubic aluminum oxynitride spinel (AlON). *J Am Ceram Soc* 1979;**62**:476–9.
8. Mitomo M, Moriyoshi Y, Sakai T, Ohsaka T, Kobayashi M. Translucent-sialon ceramics. *J Mater Sci Lett* 1982;**1**:25–6.
9. Kuramoto N, Taniguchi H. Transparent AlN ceramics. *J Mater Sci Lett* 1984;**3**:471–4.
10. DeWith G, Van Dijk HJA. Translucent $Y_3Al_5O_{12}$ ceramics. *Mater Res Bull* 1984;**19**:1669–74.
11. Lu J, Prahu M, Xu J, Ueda K, Yagi H, Yanagitani T, et al. Highly efficient 2% Nd:yttrium alumina garnet ceramic laser. *Appl Phys Lett* 2000;**77**:3707–9.
12. Li J, Wu YS, Pan YB, Liu WB, An LQ, Wang SW, et al. Solid-state-reaction fabrication and properties of high-doping Nd:YAG transparent laser ceramic. *J Chin Ceram Soc* 2007;**35**:1600–4.
13. Li J, Wu YS, Pan YB, Guo JK. Fabrication of Cr^{4+}, Nd^{3+}:YAG transparent ceramics for self-Q-switched laser. *J Non-Cryst Solids* 2006;**352**:2404–7.
14. Ikesue A, Aung YL. Synthesis and performance of advanced ceramic laser. *J Am Ceram Soc* 2006;**89**:1936–44.
15. Li J, Wu YS, Pan YB, Liu WB, Huang LP, Guo JK. Laminar structured YAG/Nd:YAG/YAG transparent ceramics for solid-state lasers. *Int J Appl Ceram Tech* 2008;**5**:360–4.
16. Cockayne B. The uses and enigmas of the Al_2O_3–Y_2O_3 phase system. *J Less-Common Met* 1985;**144**:199–206.
17. Parthasarathy TA, Mah T, Keller K. High-temperature deformation behavior of polycrystalline yttrium aluminum garnet (YAG). *Ceram Eng Sci Proc* 1991;**12**:1767–73.
18. Ikesue A, Furusato I, Kamata K. Fabrication of polycrystalline, transparent YAG ceramics by a solid-state reaction method. *J Am Ceram Soc* 1995;**78**:225–8.
19. Lee SH, Kochawattana S, Messing GL, Dumm JQ, Quarles G, Castillo V. Solid-state reactive sintering of transparent polycrystalline Nd:YAG. *J Am Ceram Soc* 2006;**89**:1945–50.
20. Li J, Wu YS, Pan YB, Liu WB, Huang LP, Guo JK. Fabrication, microstructure and properties of highly transparent Nd:YAG laser ceramics. *Opt Mater* 2008;**31**:6–17.
21. Li XD, Li JG, Xiu ZM, Huo D, Sun XD. Transparent Nd:YAG ceramics fabricated using nanosized γ-alumina and yttria powders. *J Am Ceram Soc* 2009;**92**:241–2.
22. Li YK, Zhou SM, Lin H, Hou XR, Li WJ, Teng H, et al. Fabrication of Nd:YAG transparent ceramics with TEOS, MgO and compound additives as sintering aids. *J Alloys Compd* 2010;**502**:225–30.
23. Yang H, Qin XP, Zhang J, Wang SW, Ma J, Wang LX, et al. Fabrication of Nd:YAG transparent ceramics with both TEOS and MgO additives. *J Alloys Compd* 2011;**509**:5274–9.
24. Tang F, Cao YG, Guo W, Chen YJ, Huang JQ, Deng ZH, et al. Fabrication and laser behavior of the Yb:YAG ceramic microchips. *Opt Mater* 2011;**33**:1278–82.
25. Yanagitani T, Yagi H, Ichikawa A. *Production of yttrium aluminum garnet fine powder*. Jpn Patent 10-101333; 1998.
26. Yanagitani T, Yagi H, Imagawa M. *Production of powdery starting material for yttrium aluminum garnet*. Jpn Patent 10-101334; 1998.
27. Yanagitani T, Yagi H, Yamazaki H. *Production of fine powder of yttrium aluminum garnet*. Jpn Patent 10-101411; 1998.
28. Lu J, Ueda K, Yagi H, Yanagitani T, Akiyama Y, Kaminskii AA. Neodymium doped yttrium aluminum garnet ($Y_3Al_5O_{12}$) nanocrystalline ceramics—a new generation of solid state laser and optical materials. *J Alloys Compd* 2002;**341**:220–5.
29. Liu WB, Zhang WX, Li J, Kou HM, Zhang D, Pan YB. Synthesis of Nd:YAG powders leading to transparent ceramics: the effect of MgO dopant. *J Eur Ceram Soc* 2011;**31**:653–7.
30. Wu YS, Li J, Pan YB, Guo JK, Jiang BX, Xu Y, et al. Diode-pumped Yb:YAG ceramic laser. *J Am Ceram Soc* 2007;**90**:3334–7.
31. Zhang WX, Pan YB, Zhou J, Liu WB, Li J, Jiang BX, et al. Diode-pumped Tm:YAG ceramic laser. *J Am Ceram Soc* 2009;**92**:2434–7.
32. Vrolijk JWGA, Willems JWMM, Metselaar R. Coprecipitation of yttrium and aluminium hydroxide for preparation of yttrium aluminium garnet. *J Eur Ceram Soc* 1990;**6**:47–53.
33. Sordelet DJ, Akinc M, Panchula ML, Han Y, Han MH. Synthesis of yttrium aluminum garnet precursor powders by homogeneous precipitation. *J Eur Ceram Soc* 1994;**14**:123–30.
34. Matsushita N, Tsuchiya N, Nakatsuka K, Yanagitani T. Precipitation and calcination processes for yttrium aluminum garnet precursors synthesized by the urea method. *J Am Ceram Soc* 1999;**82**:1977–84.
35. Li JG, Ikegami T, Lee JH, Mori T, Yajima Y. Co-precipitation synthesis and sintering of yttrium aluminum garnet (YAG) powders: the effect of precipitation. *J Eur Ceram Soc* 2000;**20**:2395–405.
36. Wang JQ, Zheng SH, Zeng R, Dou SX, Sun XD. Microwave synthesis of homogeneous YAG nanopowder leading to a transparent ceramic. *J Am Ceram Soc* 2009;**92**:1217–23.
37. Nyman M, Caruso J, HampdenSmith MJ. Comparison of solid-state and spray-pyrolysis synthesis of yttrium aluminate powders. *J Am Ceram Soc* 1997;**80**:1231–8.
38. Zhou YH, Lin J, Yu M, Han SM, Wang SB, Zhang HJ. Morphology control and luminescence properties of YAG:Eu phosphors prepared by spray pyrolysis. *Mater Res Bull* 2003;**38**:1289–99.
39. Pillai KT, Kamat RV, Vaigya VN, Sood DD. Synthesis of yttrium aluminum garnet by the glycerol route. *Mater Chem Phys* 1996;**44**:255–60.
40. Hakuta Y, Haganuma T, Sue K, Adschiri T, Arai K. Continuous production of phosphor YAG:Tb nanoparticles by hydrothermal synthesis in supercritical water. *Mater Res Bull* 2003;**38**:1257–65.
41. Li X, Liu H, Wang JY, Cui HM, Han F. Production of nanosized YAG powders with spherical morphology and nonaggregation via a solvothermal method. *J Am Ceram Soc* 2004;**87**:2288–90.
42. Manalert R, Rahaman MN. Sol–gel processing and sintering of yttrium aluminum garnet (YAG) powders. *J Mater Sci* 1996;**31**:3453–8.
43. Liu QM, Dong WS, Wang HJ, Wang XK. A novel way to synthesize yttrium aluminum garnet from metal-inorganic precursors. *J Am Ceram Soc* 2002;**85**:490–2.
44. Wang HM, Simmonds MC, Huang YZ, Rodenburg JM. Synthesis of nanosize powders and thin films of Yb-doped YAG by sol–gel methods. *Chem Mater* 2003;**15**:3474–80.
45. Cinibulk MK. Synthesis of yttrium aluminum garnet from a mixed-metal citrate precursor. *J Am Ceram Soc* 2000;**83**:1276–8.
46. Li J, Pan YB, Qiu FG, Wu YS, Liu WB, Guo JK. Synthesis of nanosized Nd:YAG via gel combustion. *Ceram Int* 2007;**33**:1047–52.
47. Li J, Pan YB, Qiu FG, Wu YS, Guo JK. Nanostructured Nd:YAG powders via gel combustion: the influence of citrate to nitrate ratio. *Ceram Int* 2008;**34**:141–9.
48. Chen DY, Jordan EH, Gell M. Sol–gel combustion synthesis of nanocrystalline YAG powder from metal-organic precursors. *J Am Ceram Soc* 2008;**91**:2759–62.
49. Yang L, Lu TC, Xu H, Zhang W, Ma BY. A study on the effect factors of sol–gel synthesis of yttrium aluminum garnet nanopowders. *J Appl Phys* 2010;**107**:064903.
50. Kato S, Iga T, Hatano S, Isawa Y. Synthesis of $NH_4AlO(OH)HCO_3$. *Yogyo-Kyokai-Shi* 1976;**84**:215–20.
51. Saito N, Matsuda S, Ikegami T. Fabrication of transparent yttria ceramics at low temperature using carbonate-derived powder. *J Am Ceram Soc* 1998;**81**:2023–8.
52. Sordelet DJ, Akine M. Preparation of spherical, mono-sized Y_2O_3 precursor particles. *J Colloids Int Sci* 1988;**122**:47–59.

53. Li JG, Ikegami T, Lee JH, Mori T. Low-temperature fabrication of transparent yttrium aluminum garnet (YAG) ceramics without additives. *J Am Ceram Soc* 2000;**83**:961–3.
54. Kupp ER, Messing GL, Anderson JM, Gopalan V, Dumm JQ, Kraisinger C, et al. Co-casting and optical characteristics of transparent segmented composite Er:YAG laser ceramics. *J Mater Res* 2010;**25**: 476–83.
55. Stevenson AJ, Li X, Martinez MA, Anderson JM, Suchy DL, Kupp ER, et al. *J Am Ceram Soc* 2011;**94**:1380–7.